Gallium-68 Chelate Imaging of Human Colon Carcinoma Xenografts Pretargeted with Bispecific Anti-$CD44_{V6}$/Anti-Gallium Chelate Antibodies

Gabor Klivényi, Jochen Schuhmacher, Erik Patzelt, Harald Hauser, Ronald Matys, Marion Moock, Thomas Regiert and Wolfgang Maier-Borst

Department of Diagnostic and Therapeutic Radiology, German Cancer Research Center, Heidelberg, Germany; and Department of Cell Biology, Bender & Co. GmbH, Vienna, Austria

Recently, we demonstrated the feasibility of combining improved tumor-to-tissue contrasts and PET imaging for immunoscintigraphic tumor localization using a multistep targeting technique that consists of the administration of an antitumor/antihapten bispecific monoclonal antibody (BS-MAb), a blocker to saturate the antihapten binding sites of the BS-MAb that are still present in the circulation, and a low molecular weight Ga chelate, labeled with positron emitter ^{68}Ga, serving as the hapten. Due to this technique, the biodistribution of the radiolabeled hapten is governed mainly by the binding characteristics of both the antitumor and the antihapten part of the BS-MAb. For a future clinical implementation of the method, we investigated MAb VFF18, which is reactive with the adhesion molecule $CD44_{V6}$, a tumor-associated antigen, and up-regulated in colon, squamous cell and pancreas carcinoma, and two anti-Ga chelate MAbs, which are highly selective for only one of the two enantiomers (optical isomers) of the inherently racemic Ga chelate. **Methods:** From the VFF18 MAb and the anti-Ga chelate MAbs, two BS-MAbs containing the same antitumor parts, but different antihapten parts, were prepared and tested for multistep targeting in human colon carcinoma-bearing nude mice. **Results:** Despite identical biodistributions of both BS-MAbs and their very similar affinities for the corresponding Ga chelate enantiomers, tumor uptake of the two enantiomers 1 hr postinjection was significantly different [8.7 ± 1.9% versus 5.8% ± 1.6% of the injected dose/g (%ID/g)], with tumor-to-blood ratios being higher for the BS-MAb showing the lower tumor uptake (7.6 ± 1.6 versus 4.7 ± 0.6). From data obtained with each BS-MAb, a similar initial tumor binding of ~15.5%ID/g, but different in vivo half-lives of the corresponding BS-MAb-enantiomer immune complexes, could be estimated. Pretargeting with a mixture of both BS-MAbs followed by the administration of the racemic Ga chelate resulted in the lowest tumor uptake (3.9% ± 1.5%ID/g). PET imaging of nude mice with the enantiomeric, as well as with the racemic, ^{68}Ga chelate demonstrated a clear delineation of tumors against blood pool background. **Conclusion:** Multistep immunoscintigraphy with BS-MAbs markedly increases tumor-to-tissue ratios in nude mice and enables PET imaging. Using a BS-MAb containing MAb VFF18, a more sensitive localization of $CD44_{V6}$-positive tumors in patients should also be obtained.

Key Words: immunoscintigraphy; pretargeting; bispecific antibodies; gallium-68; PET

J Nucl Med 1998; 39:1769–1776

An increase in sensitivity of immunoscintigraphic tumor localization is a prerequisite for a stronger impact of immunoscintigraphy on the therapeutical management of patients (*1–4*). A promising technique to improve sensitivity is multistep targeting using monoclonal antibodies (MAbs) additionally coupled with a high-affinity, noncovalent binding site for a small radiolabeled hapten, which is given after the localization of the MAbs in the tumor (*5*). These techniques circumvent the limitations of high blood pool and liver background activity (*6,7*), as well as of macromolecule targeting of solid tumors (*8,9*) related to the administration of MAbs labeled before injection, and allow optimization of tumor-to-normal tissue contrasts by reducing background activity (*10–13*). Besides multistep targeting techniques, PET per se, providing a better contrast resolution and a higher detection efficiency compared to conventional gamma cameras, can improve the sensitivity of immunoscintigraphic tumor localization, as demonstrated by a Phase I study comparing the ^{64}Cu-1,4,8,11 tetraazacyclotetra decane-N,N′,N″,N‴ tetraacetic acid and ^{111}In-diethylenetriamine pentaacetic acid-labeled anticolorectal carcinoma MAb 1A3 (*14*).

In a previous article (*15*), we substantiated the feasibility of combining multistep immunoscintigraphy and PET in nude mice xenografted with a rat pancreas carcinoma using bispecific antitumor/anti-Ga chelate MAbs (BS-MAbs), a blocker consisting of human apotransferrin coupled with the nonradioactive Ga chelate, to saturate anti-Ga chelate-binding sites of BS-MAbs that are still present in the circulation and the ^{68}Ga-labeled Ga chelate for tumor localization with PET. Targeting experiments with different doses of the reagents, especially of the blocker, and with different time intervals between the injections, resulted in a treatment schedule that provided an optimum tumor contrast with regard to the limited time period available for PET imaging after administration of the short-lived ^{68}Ga chelate. The results appeared to be valid for other BS-MAb/tumor models.

In this study, we included a new MAb in multistep targeting to serve as an antitumor part of the BS-MAb, which recognizes the human $CD44_{V6}$, an isoform of the adhesion molecule CD44. Additionally, we established a second anti-Ga chelate MAb with similar binding affinity but of opposite enantioselectivity to that previously used. Enantioselectivity for only one of the enantiomers (optical isomers) is an inherent feature of anti-chelate MAbs raised against a racemic metal chelate of high kinetic stability in vivo. Pretargeting with BS-MAbs containing a mixture of both anti-Ga chelate MAbs and administration of the racemic ^{68}Ga chelate was investigated as a substitute for using only one anti-Ga chelate MAb and the corresponding enantiomer prepared by optical resolution of the racemic chelate on an immunoadsorption column.

MATERIALS AND METHODS

Monoclonal Antibodies, Fragments and Bispecific Antibodies

Anti-Ga chelate MAbs were raised by immunization of BALB/c mice with Ga-N,N′-[2-hydroxy-5-(ethylene-β-carboxy)benzyl]eth-

Received Sep. 8, 1997; revision accepted Dec. 19, 1997.

For correspondence or reprints contact: Jochen Schuhmacher, MD, Department of Diagnostic and Therapeutic Radiology, German Cancer Research Center, Im Neuenheimer Feld 280, D-69120 Heidelberg, Germany.

ylene diamine N,N′-diacetic acid (HBED-CC) coupled to keyhole limpet hemocyanin as described previously (*16*). The hybridomas obtained secreted MAbs of high enantioselectivity because of the racemic nature and the high kinetic stability of the Ga-HBED-CC chelate in vivo. As a counterpart to MAb 3A10 (IgG3), used in the previous studies, MAb 8-16 (IgG1), of similar affinity but of opposite enantioselectivity, was chosen. MAb 3A10 binds to the enantiomer not reactive with 8-16 and vice versa. Hybridomas were cultured in a hollow fiber reactor (Cell Pharm II; Digitana, Hamburg, Germany). MAbs were purified by affinity chromatography on protein A-Sepharose (Pharmacia, Freiburg, Germany).

Anti-$CD44_{V6}$ MAb VFF18 (IgG1) was raised by immunization of BALB/c mice with a fusion protein containing the extracellular region encoded by $exon_{V6}$ (*17*). $CD44_{V6}$ is up-regulated in several types of cancer, especially in pancreatic adenocarcinoma, squamous cell carcinoma and colon carcinoma (*17–19*). Variant isoforms of CD44 are generated by alternative splicing of at least 10 variant exons and show additional sequences near the membrane-proximal extracellular region, which are not expressed in the standard isoform $CD44_S$ of hematopoietic cells (*20*).

$F(ab)_2$ fragments of VFF18 were prepared by digestion with thiol-free, preactivated papain (5% papain, pH 5.5, 37°C, 160 min) (*21*). MAbs 3A10 and 8-16 were fragmented to $F(ab)_2$ by pepsin (2% pepsin, pH 4.5, 25°C, 45 min; and 3% pepsin, pH 3.8, 37°C, 90 min, respectively) (*22*). Fragments were purified by gel filtration on a Superdex 200 column (1.6 × 150 cm; Pharmacia) operated with 0.65 *M* NaCl-0.1 *M* phosphate buffer, pH 7.3, and a flow rate of 0.2 ml/min.

The preparation of BS-MAbs via a mixed functional chemical linker has been described previously (*15*). Briefly, VFF18 $F(ab)_2$ fragments were incubated with *N*-hydroxysuccinimidyl-6-maleimidocaproate (EMCS; Calbiochem, Bad Soden, Germany) in a molar ratio of 3.5:1. To the EMCS-derivatized $F(ab)_2$, a 2-fold molar excess of 3A10 or 8-16 F(ab′) was added, which had been prepared by reducing the corresponding $F(ab')_2$ with dithiothreitol (Sigma, Munich, Germany). The mixtures were purged with argon and allowed to react for 24 hr at room temperature. The $F(ab)_2$/F(ab′) BS-MAbs with an apparent M_r of 160,000 were separated on a Sephadex column as described for $F(ab)_2$ purification.

Tumors

For all in vitro and in vivo studies, the tumor cell line HT29, derived from a human colon carcinoma, was used (*23*). Expression of $CD44_{V6}$ by HT 29 cells was demonstrated by reverse-transcribed polymerase chain reaction analysis (*24*). Cells were grown in RPMI 1640 medium supplemented with 10% fetal calf serum and harvested by trypsination.

Gallium-67/68-N,N′-[2-Hydroxy 5-(Ethylene-β-Carboxy)Benzyl]Ethylene Diamine N,N′-Diacetic Acid Chelate

The ligand HBED-CC was synthesized by a Mannich reaction starting with 3(p-hydroxyphenyl) propionic acid and ethylene diamine N,N′-diacetic acid as described previously (*16*). To 20 μl of ^{67}Ga (~110 MBq in 0.4 *N* HCl; Mallinckrodt, Hennef, Germany), 4 μl of 1 m*M* inactive Ga^{3+} in 0.1 *N* HCl, 5 μl of 1 m*M* aqueous HBED-CC solution and 200 μl of 0.1 *M* acetate buffer (pH 4.8) were added. The mixture was adjusted to pH 4.8 with 0.1 *N* NaOH and kept for 25 min at 95°C in a water bath. After neutralization to pH 7.0, the mixture was given on a cation exchange column (0.5 × 3.0 cm; Chelex 100, Bio-Rad, Munich, Germany). An excess of ^{67}Ga was retained on the resin, whereas ^{67}Ga-HBED-CC quantitatively appeared in the effluent. Gallium-68 (925 MBq) was obtained in 0.3 ml of 0.5 *N* HCl from a ^{68}Ge/^{68}Ga generator (*25*). After the addition of 2 μl of 1 m*M* Ga^{3+} solution, the mixture was evaporated to dryness and redissolved in 200 μl of acetate buffer (pH 4.8). All subsequent steps were identical to that of ^{67}Ga labeling. For resolution of the racemic Ga chelate into its enantiomers, immunoadsorption columns containing either 3A10 or 8-16 immobilized to Sepharose (1 × 6 cm, 2.5 mg MAb/ml Sepharose) were used. The Chelex effluent (~1.5 ml), containing up to 100 nmol of racemic chelate, was added to the column and eluted with 0.01 *M* phosphate-buffered saline (PBS) at a flow rate of 1.5 ml/min.

Gallium-N-[2-Hydroxy-5-(Ethylene-β-Carboxy)Benzyl] N′-[2-Hydroxy-5-(Ethylene-β-Isothiocyanato)Benzyl]Ethylene Diamine N,N′ Diacetic Acid (HBED-CI) Transferrin (Blocker)

The synthesis, biodistribution and competition of the blocker with the free Ga chelate for BS-MAb-binding sites have been described previously (*15*). Briefly, human apotransferrin (Sigma) was reacted with the ligand HBED-CI, a derivative containing one carboxyl and one isothiocyanate group, in a molar ratio of 1:75. Subsequently, the conjugate was saturated with Ga^{3+} labeled with a small amount of ^{67}Ga to serve as a tracer for Ga^{3+} incorporation. The blocker reduced binding of the free ^{67}Ga chelate to BS-MAbs in the circulation by a factor of 10 and showed a blood clearance much faster than that of unsubstituted transferrin, with the hepatobiliary system as the main route of excretion.

Iodine Labeling of Monoclonal Antibodies

Protein solutions (5–10 mg/ml in 0.05 *M* PB) were placed in glass tubes coated with 20 μg of IODO-GEN (Pierce, Rockford, IL) per mg of protein. After the addition of ^{125}I-iodide (3.7 GBq/ml; Amersham Buchler, Braunschweig, Germany) the reaction was continued for 10 min at room temperature. Labeled proteins were separated from free iodine by a centrifuged column procedure using Bio-Gel P30 (Bio-Rad) preloaded with 0.01 *M* PBS. Specific activities of MAbs were adjusted at 15–20 KBq/1 μg.

In Vitro Assays

The immunoreactive fractions (IFs) of VFF18, VFF18 $F(ab)_2$ and BS-MAbs toward HT29 tumor cells were determined using the Lineweaver-Burk approach, as modified by Lindmo et al. (*26*). One million cells suspended in 150 μl of RPMI 1640 and 1% bovine serum albumin were serially diluted by a factor of 2 and were incubated with a fixed amount of 10 ng of the ^{125}I-labeled MAbs for 2 hr at 37°C. Cells were washed three times, and radioactivity in the cell pellet was counted. A least squares fit from a plot of total activity added/activity bound to cells versus the inverse of cell concentration results in a straight line showing an intercept with the total activity added/activity bound to cells axis, which represents the inverse of the IF.

Equilibrium binding (K) was determined using a fixed number of 1×10^6 cells and increasing amounts (10–320 ng) of labeled MAbs. A least squares fit from a Scatchard plot [bound activity/free activity (B/F) versus bound activity (B)] gives a straight line, the slope of which indicates K. The data of K were corrected for the immunoreactive fraction according to Badger et al. (*27*). The intercept of B/F with B represents the maximum concentration of MAb-binding sites.

K and IF of 3A10 and 8-16 MAbs, fragments and BS-MAbs with the Ga chelate were determined by ammonium sulfate (AS) precipitation of the MAb/Ga chelate immune complexes. Twenty nanograms of ^{125}I-labeled MAbs were incubated with increasing amounts 0.075–1.2 ng (0.125–2.0 pmol) of enantiomeric ^{67}Ga-HBED-CC in a total volume of 1 ml PBS containing 1 mg BSA and 1.5 mg pig IgG and kept for 2 hr at 37°C. After addition of 1 ml saturated AS solution, precipitation was completed in 7 min at 4°C. Precipitates were centrifuged and washed twice with 2 ml of half-saturated AS. A Scatchard plot of B/F versus B indicates K.

The intercept with the B-axis represents the maximum amount of Ga chelate bound to MAbs at infinite Ga chelate excess. Immunoreactive fraction is calculated from the measured and the theoretical saturation of the MAbs added.

Dissociation

Dissociation of the BS-MAb/Ga chelate immune complexes was determined via a cell assay. HT29 tumor cells (2×10^6) were incubated with 40 ng (0.25 pmol) of ^{125}I-labeled BS-MAb and 0.15 ng (0.25 pmol) of enantiomeric ^{67}Ga-HBED-CC for 2 hr at 37°C in a volume of 200 μl of RPMI 1640 plus fetal calf serum. Subsequently, cells were separated from the incubation mixture, washed three times and resuspended in 200 μl of medium supplemented with 30 μg (50 nmol) unlabeled racemic Ga-HBED-CC and kept at 37°C. At time intervals up to 90 min, duplicate samples were washed and counted for cell-bound ^{67}Ga and ^{125}I activities. Gallium-67 chelate binding was normalized for the amount of BS-MAbs bound to cells and corrected for unspecific ^{67}Ga-HBED-CC absorption.

Animal Experiments

In biodistribution experiments, we used 6- to 8-wk-old female CD1 *nu/nu* mice (IFA CREDO, L'Arbresle, France); all were reared under special pathogen-free conditions. Nude mice were inoculated subcutaneously with 1.5×10^6 HT29 tumor cells (in 0.2 ml of RPMI 1640) in the flank near the shoulder. Four weeks later, tumors with a weight of 100–650 mg were selected for the experiments. Mice were given injections into the tail vein of 200 μl of PBS containing 10 μg of human serum albumin and the labeled compounds under investigation. At the time points indicated, animals were anesthetized with ether, bled from the retroorbital plexus and killed by cervical dislocation. Organs were removed, weighed and counted for radioactivity.

Biokinetics of MAbs and fragments were determined in tumor-bearing mice after injection of 15 μg (100 pmol) of ^{125}I-VFF18 MAb, 11 μg (100 pmol) of ^{125}I-VFF18 F(ab)$_2$, 16 μg of (100 pmol) ^{125}I-VFF18 F(ab)$_2$/3A10 F(ab') BS-MAb or 16 μg (100 pmol) of ^{125}I-VFF18 F(ab)$_2$/8-16 F(ab') BS-MAb. Animals were examined at 1, 24, 48 and 72 hr for MAbs and at 1, 6, 18, 24 and 48 hr for F(ab)$_2$ and BS-MAbs.

Targeting experiments with the ^{67}Ga chelate were performed with the same treatment schedule as described previously (*15*). Tumor-bearing mice were preinjected with 16 μg (100 pmol) ^{125}I-VFF18/3A10, 16 μg VFF18/8-16 or a mixture containing 8 μg of each BS-MAb and blocked 18 hr later by the administration of 8.6 μg (100 pmol) of Ga chelate-modified transferrin. Fifteen minutes after the blocker, 9.6 ng (16 pmol) of either racemic ^{67}Ga-HBED-CC or the corresponding enantiomer were administered. Animals were examined 1 hr after the chelate administration.

Scintigraphy

PET imaging was performed with a two-ring detector system (PC 2048-7 WB, Scanditronix). Three slices, two primary sections and one cross-section, with thicknesses of 11, 8 and 11 mm, respectively, were generated using an improved version of an iterative reconstruction algorithm (*28*). The pixel size was 1 mm^2, and resolutions obtained were 2.5 mm transaxial and 8–11 mm axial. Female tumor-bearing mice were given injections of 9.6 ng (16 pmol) of the ^{68}Ga chelate (90 KBq ^{68}Ga/ng) and imaged 1 hr postinjection. Animals were pretreated with BS-MAbs and blocker as described. A total of $4–5 \times 10^5$ counts were acquired within 30 min. The three slices of an image were scaled to the same maximum. Animals were killed 5 min before acquisition, and transmission measurements were performed 4–5 hr later, when most of the ^{68}Ga activity was decayed. Subsequently, tumors were removed, weighed and counted for ^{125}I and ^{68}Ga activities.

TABLE 1
Immunoreactive Fraction (IF) and Equilibrium Binding (K) of Antitumor (VFF18) and Antichelate (3A10; 8–16) Monoclonal Antibodies

MAb	IF (%)	K (M^{-1})
VFF18*	74.6†	3.40×10^{9}†‡
VFF18 F(ab)$_2$*	71.7	2.86×10^{9}
VFF18/3A10 BS-MAb*	73.0	1.82×10^{9}
VFF18/8-16 BS-MAb*	61.9	1.96×10^{9}
3A10§	71.4	1.84×10^{10}
3A10 F(ab)$_2$§	80.9	1.65×10^{10}
VFF18/3A10 BS-MAb§	79.1	2.18×10^{10}
8-16§	95.1	1.64×10^{10}
8-16 F(ab)$_2$§	91.7	1.43×10^{10}
VFF18/8-16 BS-MAb§	91.0	1.64×10^{10}

*IF and K determined with the human colon carcinoma cell line HT29.
†Correlation coefficient r for all Scatchard and Lineweaver-Birk plots ≥0.94.
‡Binding constants are corrected for IF according to Badger et al. (27).
§IF and K determined with ammonium sulphate precipitation of the enantiomeric Ga-HBED-CC/MAb immune complexes.

RESULTS

Reagents

F(ab)$_2$ fragments used as the starting material for BS-MAb preparation were of high purity. From sodium dodecyl sulfate-polyacrylamide gel electrophoresis, it was estimated that >90% of the proteins migrated as band with an apparent M_r of 110,000. The Superdex column effectively separated the desired 160-kDa F(ab)$_2$/F(ab)' BS-MAbs from unreacted F(ab)$_2$ and F(ab') as well as from 210- and 260-kDa conjugates containing two or three F(ab') per F(ab)$_2$.

Preparation of the $^{67/68}$Ga-HBED-CC chelate was performed with a slight excess of Ga^{3+} carrier assuring a complete 1:1 stoichiometric saturation of the ligand by the metal ion and was followed by the retention of uncomplexed Ga^{3+} on a Chelex column. The necessary amount of Ga^{3+} carrier, depending on the metal impurities in the $^{67/68}$Ga radionuclide preparations, was determined experimentally. The effluent was checked by paper chromatography (Whatman no. 1; Whatman, Clifton, NJ; methanol/water, 5.5:4.5). Typically, >99% of the radioactivity migrated with an R_f of 0.7 corresponding to the Ga chelate. Separation of the racemic Ga chelate into its enantiomers by means of immunoadsorption took 15 min. The enantiomers eluted at 9–13 ml; yield and purity, as checked by AS precipitation with the corresponding antichelate MAb, were >90%. Starting with 925 MBq of ^{68}Ga, 2 nmol of Ga^{3+} carrier, 5 nmol of ligand and an overall preparation time of ~75 min, a total of 2.4 nmol of enantiomer with a specific activity of ~81 MBq ^{68}Ga/nmol Ga chelate (= 135 MBq/μg) could be obtained.

Synthesis of the blocker resulted in a final product containing an average of 15 molecules of Ga chelate per molecule of transferrin. Because of the racemic nature of the transferrin-bound Ga chelate, the blocker effectively competes with both enantiomers of the free, radiolabeled Ga chelate for binding with the corresponding antichelate MAbs.

In Vitro Assays

The IF and equilibrium binding (K) of antitumor and anti-Ga chelate MAbs were determined from Lineweaver-Burk and Scatchard plots with data obtained from HT29 cell assays or by AS precipitation of the enantiomeric Ga chelate/MAb immune complexes (Table 1). Equilibrium binding of the F(ab)$_2$ frag-

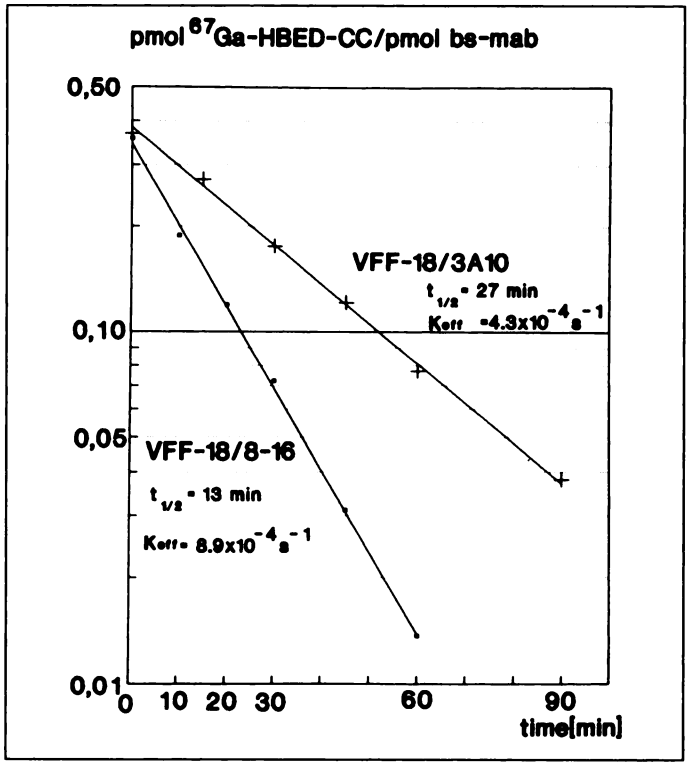

FIGURE 1. Semilogarithmic plot of in vitro dissociation of enantiomeric ^{67}Ga-HBED-CC from corresponding BS-MAbs bound to HT29 cells. Data are normalized for the amount of BS-MAbs bound to cells.

ment of VFF18 measurably decreased after BS-MAb preparation, probably due to a coupling of the linker EMCS with an amino group near the binding sites of the fragment. No such decrease was found for both antichelate MAbs, the F(ab') fragments of which react via a SH group of the hinge region, far away from the binding site. BS-MAb preparation had no effect on IF of the VFF18 or antichelate MAbs. From Scatchard plots of VFF18 binding to HT29 tumor cells, a maximum of ~0.9 × 10^5 MAbs/cell was estimated.

In vitro dissociation was calculated from the displacement of enantiomeric ^{67}Ga-HBED-CC at 37°C from the cell-bound BS-MAbs by a 2 × 10^5-fold molar excess of racemic, nonradioactive Ga chelate. Data resulted in monoexponential curves corresponding to dissociation half-lives of 27 ± 3.0 and 13 ± 1.7 min for the 3A10- and 8-16-containing BS-MAb immune complexes, respectively (Fig. 1). Dissociation at 4°C increased half-lives by a factor of 9 (data not shown). For comparison, all in vitro tests with 8-16 and 3A10 antichelate MAbs and the corresponding, enantiomeric Ga chelate were repeated with twice the amount of racemic Ga chelate. Virtually no difference in the stoichiometric uptake of racemic or enantiomeric Ga chelate by the MAbs was noted.

In Vivo Studies

Biodistributions of ^{125}I-labeled VFF18 MAb, VFF18 F(ab)$_2$ and VFF18 F(ab)$_2$/3A10 F(ab') BS-MAb in tumor-bearing nude mice are presented in Figure 2. Data of VFF18/8-16 BS-MAb (data not shown) were identical to those of VFF18/3A10 BS-MAb. Tumor uptake of the native MAb increased to about 13%ID/g and then remained nearly constant for the time period investigated. Maximum BS-MAb accumulation in the tumor was lower and amounted to 9.5% ± 1.8%ID/g, but it was achieved earlier with a peak at about 18 hr. Peaking of the BS-MAb concentration in the tumor appears to be a consequence of a markedly accelerated BS-MAb blood clearance, which is due to the lack of a Fc-part in the BS-MAb molecule.

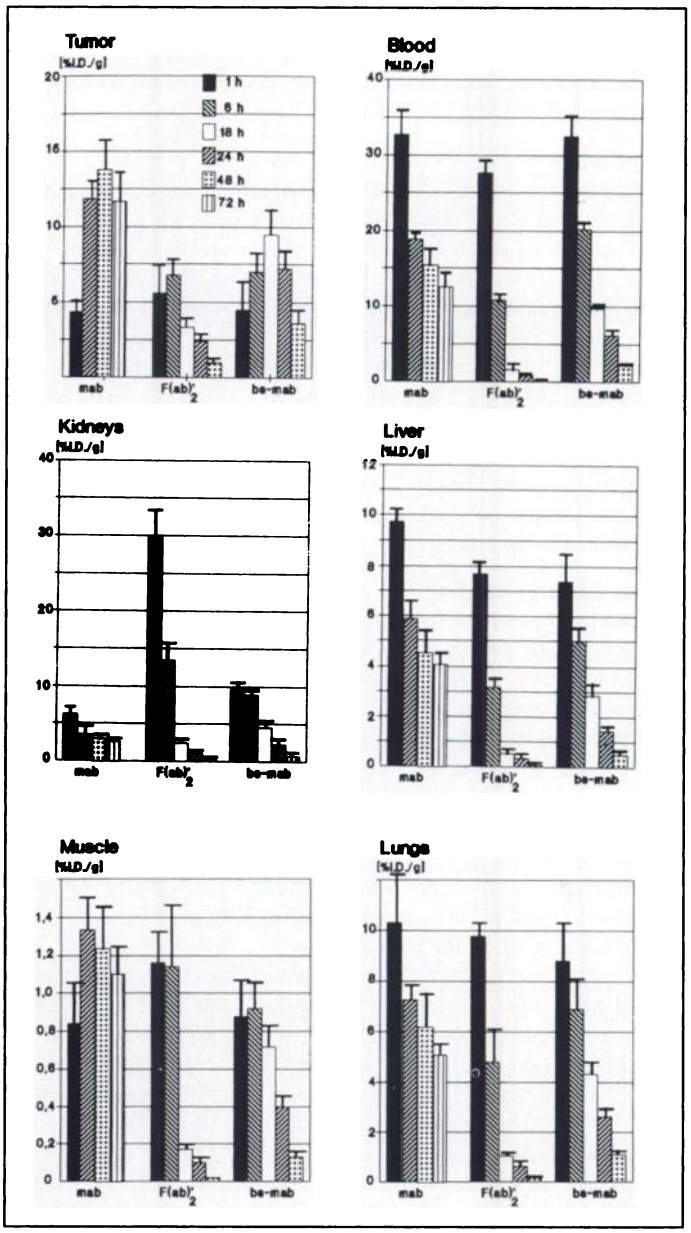

FIGURE 2. Biokinetics of ^{125}I-labeled VFF18 MAb, VFF18 F(ab)'$_2$ and VFF18/3A10 BS-MAb in HT 29 tumor-bearing nude mice. Animals were given intravenous injections of 15 μg (100 pmol) of MAb, 11 μg (100 pmol) of F(ab)'$_2$ or 16 μg (100 pmol) of BS-MAb. Data are the means ± s.d. (n = 5). The mean body weight of the animals was 23.1 ± 1.6 g, the liver weight was 1.33 ± 0.11 g, the weight of both kidneys was 0.43 ± 0.03 g, the weight of the lungs was 0.17 ± 0.03, the spleen weight was 0.14 ± 0.05 g and tumor weight was 0.30 ± 0.20 g (range 0.09–0.82 g; n = 70).

Thus, the kinetics of the 160-kDa BS-MAb in tumor, blood and most other tissues are more similar to those of the 110 kDa F(ab)$_2$ than to those of the 150-kDa native MAb, with the exception of the high renal F(ab)$_2$ uptake 1 hr postinjection, which was not observed for BS-MAbs and the native MAb. For further experiments with blocker and ^{67}Ga chelate a localization period of 18 hr for the BS-MAbs was chosen, showing the maximum tumor uptake of 9.5 ± 1.8%ID/g and a 1:1 tumor-to-blood ratio.

Targeting with enantiomeric or racemic ^{67}Ga chelate was performed in tumor-bearing mice pretreated with ^{125}I-labeled BS-MAbs and blocker. Biodistribution data of the ^{67}Ga chelate and the ^{125}I-BS-MAbs measured simultaneously are presented in Figure 3. The highest tumor uptake (8.7 ± 1.9%ID/g 1 hr p.i.) was obtained for the enantiomeric ^{67}Ga chelate reactive

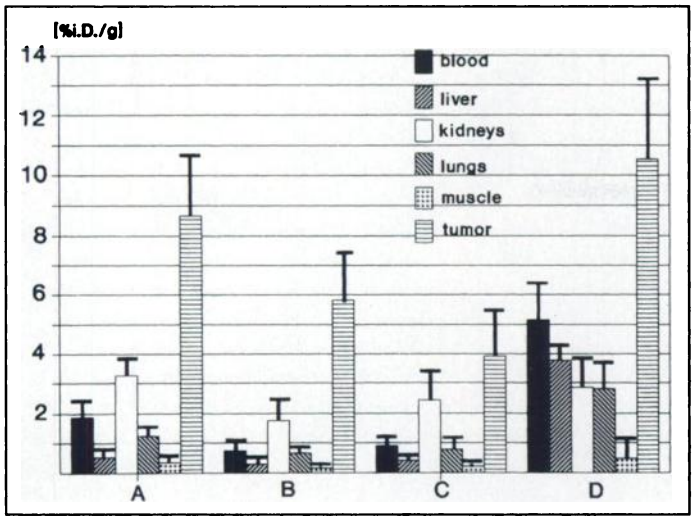

FIGURE 3. Biodistribution of ^{125}I-labeled BS-MAbs and of enantiomeric or racemic ^{67}Ga-HBED-CC in tumor-bearing nude mice after multistep targeting. Schedule: 100 pmol of BS-MAbs; 18 hr later, 100 pmol of blocker; 15 min later, 16 pmol of ^{67}Ga chelate; 1 hr later, examination. Data are the means ± s.d.. (A) VFF18/3A10 BS-MAb; Λ enantiomer of ^{67}Ga chelate (n = 6). (B) VFF18/8-16 BS/MAb; Δ enantiomer of ^{67}Ga chelate (n = 6). (C) A 1:1 mixture of VFF18/3A10 and VFF18/8-16 BS/MAb; racemic ^{67}Ga chelate (n = 6). (D) Iodine-125 BS-MAbs (n = 18). Because biodistribution of the different BS-MAbs were identical, data for animals of Groups A–C are combined. The designations Λ and Δ for corresponding enantiomers are not definitive. Body weight and organ weights of animals were similar to those in Figure 2. Tumor weight, 0.26 ± 0.16 g; range 0.07–0.54 g.

with the 3A10 containing BS-MAb (Fig. 3A), whereas tumor concentration of the opposite enantiomer reactive with the 8-16 containing BS-MAb was significantly lower (5.8% ± 1.6%ID/g; $p \leq 0.05$; Fig. 3B). Tumor uptake of the racemic ^{67}Ga chelate after pretreatment with the BS-MAb mixture was expected to be the arithmetic mean (7.3%ID/g) but amounted to only 3.9 ± 1.5%ID/g, approximately half the expected value (Fig. 3C). Administration of the blocker not only reduced ^{67}Ga activity in the blood by saturation of the antichelate binding sites of BS-MAbs present in the circulation but also significantly reduced BS-MAb concentration by a factor of 2 (Fig. 3D; see Fig. 2, blood, BS-MAb 18 hr). As determined previously, biodistribution of the ^{67}Ga chelate in animals not pretreated with BS-MAbs showed <0.15%ID/g in all tissues 1 hr postinjection. Pretreatment with a 3A10 containing BS-MAb, but without the administration of the blocker, resulted in a ^{67}Ga chelate uptake of 4% and 27%ID/g 1 hr postinjection in tumor and blood, respectively, indicating a strong trapping of the free ^{67}Ga chelate by BS-MAb in the circulation and only a small fraction capable of penetrating the pretargeted tumor tissue (*15*).

Tumor-to-tissue ratios obtained for the enantiomeric ^{67}Ga-HBED-CC behave in an opposite manner compared with tumor uptake, showing a higher contrast for the enantiomer reactive with the 8-16 containing BS-MAb despite its lower tumor accumulation (Table 2). Compared with the native VFF18 and BS-MAbs, with or without administration of blocker, tumor to blood or liver ratios are markedly increased for either racemic or enantiomeric ^{67}Ga-HBED-CC.

Scintigraphy

PET images of tumor-bearing mice obtained with enantiomeric or racemic ^{68}Ga-HBED-CC after multistep targeting are presented in Figure 4 (A–D). The corresponding data of tumor uptake are shown in Table 3. All tumors imaged either transversally or sagittally are present in the first (upper) slices. The enhanced activity observed in normal tissues is related to urethra, bladder and kidneys. Multistep targeting of animals with VFF18/3A10 BS-MAb and the corresponding enantiomeric ^{68}Ga chelate resulted in the highest ^{68}Ga uptake with a clear delineation of tumors against the blood-pool background (Fig. 4A). Administration of a mixture of BS-MAbs and the racemic ^{68}Ga chelate led to a reduced sensitivity of tumor localization, especially of smaller tumors with a ^{68}Ga-uptake below the mean observed in biodistribution experiments (Fig. 4B). Imaging with the VFF18/8-16 BS-MAb and the corresponding enantiomeric ^{68}Ga chelate (Fig. 4C) effected the highest tumor to tissue contrasts, which, however, are not readily recognized compared to Figure 4A. The benefit of a high contrast is more evident at low counting rates, as demonstrated by the central animal in Figure 4C, which was given only half the specific activity compared to all other animals. Imaging with an appropriate scaling indicated no loss in quality of tumor localization (Fig. 4D).

TABLE 2
Tumor-to-Tissue Ratios of Iodide-125-Labeled VFF18 and of Enantiomeric or Racemic Gallium-67-HBED-CC in Nude Mice

	^{125}I-VFF18			^{67}Ga-HBED-CC		
Tumor/organ	MAb 24 hr (n = 5)	BS-MAb* 18 hr (n = 5)	BS-MAb† and blocker 19.25 hr (n = 18)	Λ enantiomer‡ 1 hr (n = 6)	Δ enantiomer§ 1 hr (n = 6)	Racemic¶ 1 hr (n = 6)
Blood	0.7 ± 0.1**	1.0 ± 0.2	2.1 ± 0.5††	4.7 ± 0.6	7.6 ± 1.6§§	4.4 ± 0.9
Liver	2.1 ± 0.3	3.4 ± 0.6	3.0 ± 0.7	15.1 ± 2.1	19.9 ± 6.7	9.4 ± 1.6
Spleen	3.2 ± 0.7	4.0 ± 0.5	5.0 ± 1.0	19.0 ± 5.0	26.9 ± 12.6	14.3 ± 4.0
Kidneys	3.2 ± 0.4	2.6 ± 0.6	4.2 ± 1.4	2.7 ± 0.6	3.5 ± 1.4	1.7 ± 0.5
Muscle	9.2 ± 1.1	13.3 ± 2.5	22.4 ± 7.1††	23.6 ± 4.5	35.6 ± 9.7	18.3 ± 4.5
Bone	6.2 ± 1.5	8.2 ± 2.1	11.7 ± 3.8	14.4 ± 4.5	18.4 ± 6.8	8.9 ± 4.4
Lungs	1.7 ± 0.1	2.2 ± 0.5	4.0 ± 1.1††	6.7 ± 0.4	8.9 ± 1.8§§	5.2 ± 1.0

*VFF 18/3A10BS-MAb.
†Because biodistributions of the different BS-MAbs were identical, data are a combination of VFF 18/3A10. VFF 18/8-16 and the 1:1 mixture of both MAbs.
‡Animals preinjected with VFF 18/3A10 BS-MAb and blocker.
§Animals preinjected with VFF 18/8-16 BS-MAb and blocker.
¶Animals preinjected with 1:1 BS-MAb mixture and blocker.
**All data are the mean ± 1 s.d.
††Significantly different ($p \leq 0.01$) from BS-MAb without administration of blocker.
§§Significantly different ($p \leq 0.01$) from Λ enantiomer. Designations Λ and Δ are not definitive.

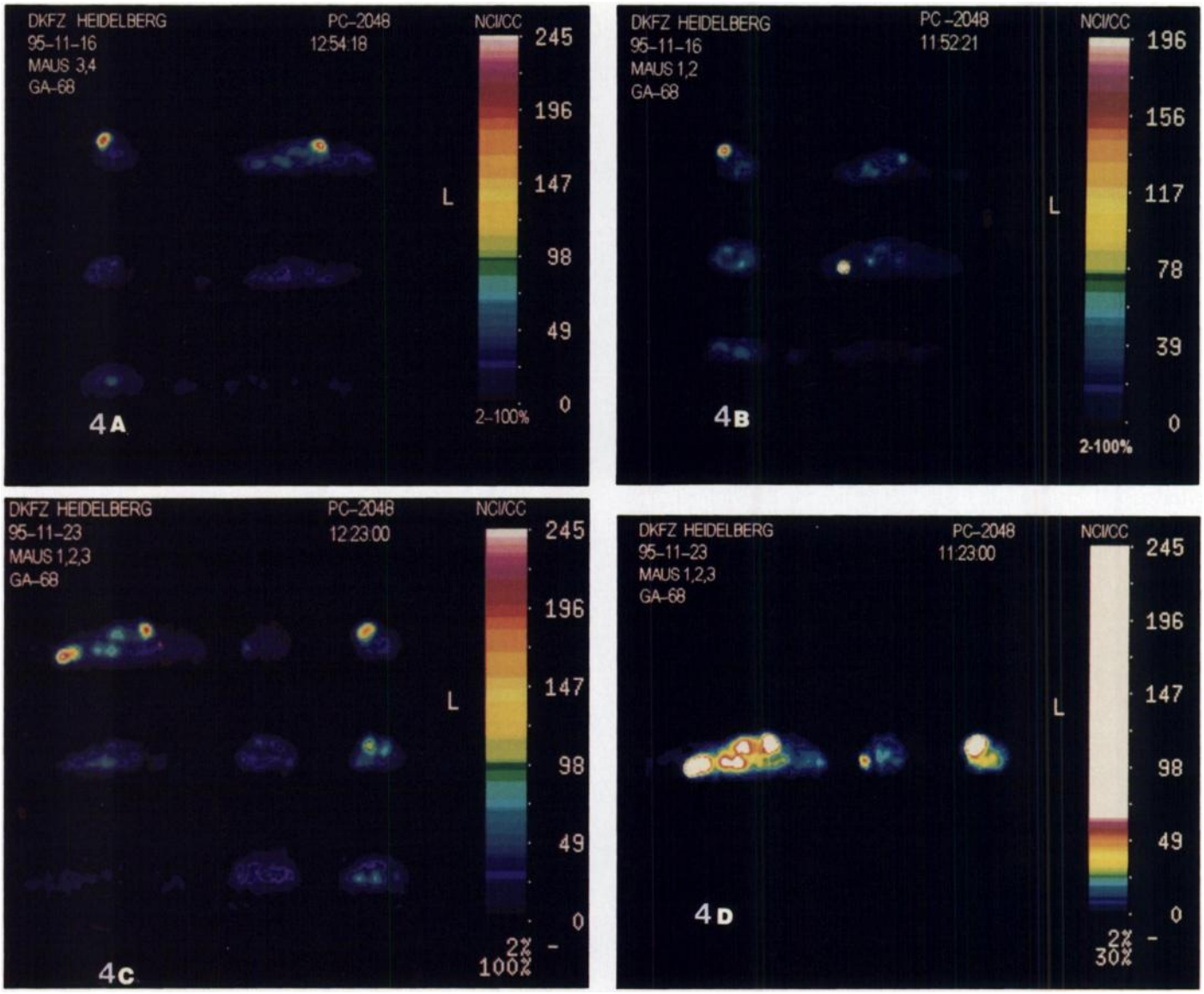

FIGURE 4. Scatter- and attenuation-corrected PET images of HT29 tumor-bearing nude mice 1 hr postinjection of 9.6 ng (16 pmol) of ^{68}Ga-HBED-CC (90 KBq/ng). Animals were preinjected with BS-MAb and blocker. (A) VFF18/3A10 BS-MAb, blocker, Λ enantiomer of the ^{68}Ga chelate. (B) Mixture of VFF18/3A10 and VFF18/8-16 BS-MAbs, blocker, racemic ^{68}Ga chelate. (C) VFF18/8-16 BS-MAbs, blocker, Δ enantiomer of the ^{68}Ga chelate. Note that the central animal received a ^{68}Ga chelate with only half the specific activity (45 KBq ^{68}Ga/ng). (D) Same as c but with a reduced scaling. For tumor uptake of radioactivity and tumor weights see Table 3.

DISCUSSION

Multistep targeting in human colon carcinoma bearing nude mice with the VFF18/3A10 BS-MAb, a blocker and the corresponding, enantiomeric $^{67/68}$Ga-HBED-CC chelate resulted in high contrast PET images 1 hr postinjection and biodistribution data, which confirm those previously obtained in a rat pancreas carcinoma with the 1.1 ASML/3A10 BS-MAb, indicating a general applicability of the method for immunoscintigraphic tumor localization simply by replacing the $F(ab)_2$ antitumor part of the BS-MAb.

However, a substitution of the 3A10 F(ab′) antichelate part of the BS-MAb by 8-16 F(ab′) resulted in a measurable lower tumor uptake of the enantiomeric counterpart but in higher tumor-to-tissue ratios 1 hr postinjection. Because of identical biodistributions of the 3A10- or 8-16-containing BS-MAbs and their nearly equal affinities for the corresponding enantiomeric

TABLE 3
Tumor Uptake of Iodine-125-BS-MAbs and Gallium-68-HBED-CC in Mice Imaged with PET

	Fig. 4A		Fig. 4B		Fig. 4C		
	Transverse	Sagittal	Transverse	Sagittal	Sagittal	Transverse	Transverse
BS-MAb (%ID/g)	11.8	9.2	10.7	8.9	14.6	7.3	10.4
Ga-chelate (%ID/g)	7.1	11.1	4.0	2.9	8.4	5.0*	4.8
Tumor weight (mg)	480	260	310	180	260	140	670

*This animal was given only half the specific activity (45 kBq of ^{68}Ga/ng Ga-chelate).

Ga chelate, a quite similar, initial binding of the radiolabeled enantiomers, but different in vivo half-lives, are suggested. Using in vivo half-lives of the enantiomeric Ga chelate/3A10 immune complex of 80 and 40 min in tumor and blood, respectively, as determined previously (*15*), and half-lives of 40 and 20 min for the 8-16-containing immune complex, concluded from its twofold in vitro dissociation rate compared to the 3A10 complex, an initial binding of ~15.5%ID/g in tumor and of 5.5%ID/g (~10%ID/organ) in blood for both enantiomers is calculated. Thus, presaturation of BS-MAb antichelate binding sites in the circulation (~18 pmol, 18 hr postinjection) by 100 pmol of blocker containing 750 pmol of each Ga chelate enantiomer reduced the initial binding of the free, enantiomeric ^{67}Ga chelate to ~10%ID (1.6 pmol), corresponding to an ~9% saturation of binding sites. The initial fraction of saturated antichelate binding sites in the tumor was nearly threefold higher, 2.5 pmol of ^{67}Ga chelate versus 9.5 pmol of BS-MAb/g tissue. Whether this fraction is limited only by the perfusion of the tumor tissue or additionally by small amounts of blocker extravasated into tumor tissue could not be determined. The different dissociation rates of the monovalent immune complexes despite nearly identical affinities may be explained by a difference in the composition of the various MAb/hapten binding forces, which are the sum of ionic interactions, hydrogen bonding and van der Waals attractions with fast kinetics on the one hand and hydrophobic bonding with slow kinetics on the other hand (*29*).

The reduced tumor uptake of racemic ^{67}Ga-HBED-CC after pretargeting with a mixture of the 3A10- and 8-16-containing BS-MAbs is not readily understood. An activity retention about half the expected value suggests a 1:1 competition of both enantiomers with each other for the same antichelate binding site, which, however, was not observed after a 2-hr incubation with the racemic Ga chelate in the in vitro assays. A hypothetic explanation might be a short-term competition of the enantiomers, caused by their identical size, molecular weight and charge distribution, dominating during the short time period available for MAb/hapten binding in vivo, while at longer reaction times in vitro, binding is governed by the highly different affinities of the enantiomers for either the 3A10 or 8-16 binding sites. Thus, with regard to tumor uptake, the substitution of enantiomeric by racemic Ga chelate, which circumvents the 50% loss of ^{68}Ga activity during optical resolution, was less favorable.

After the hypothesis described above, an improvement of the racemic Ga chelate uptake in tumors after pretargeting with a mixture of BS-MAbs of opposite enantioselectivity might be accomplished using bivalent haptens, e.g., two Ga chelate molecules covalently coupled by a chemical linker. A weak, competitive binding of the first enantiomer, although of short duration, should enhance the probability for a strong binding of the coupled second enantiomer. Additionally, bivalent MAb/hapten binding decreases the dissociation rate compared to monovalent binding, resulting in an elongated biological half-life of the bivalent hapten, especially in the nonblocked tumor tissue (*30*). With the $F(ab)_2$ antitumor/F(ab') antichelate BS-MAbs, used in our study, binding of bivalent haptens should effect a bridging of two BS-MAb molecules bound to the cell surface similar to that described by Le Doussal et al. (*11*), decreasing not only the BS-MAb/chelate, but also the BS-MAb/antigen dissociation rate, and giving rise for a tumor half-life of bivalent haptens, which may also be sufficient for a radioimmunotherapy application.

The VFF18 MAb, included in this study, targets the human $CD44_{V6}$, whose murine homolog has recently been shown to render nonmetastatic rat pancreas tumor cells metastatic (*31*). Screening of human tumors for expression of $CD44V_6$ has not yet been finished. Its potential to indicate a poor prognosis, similar to that in the rat pancreas carcinoma model, has been established for non-Hodgkin's lymphomas (*32*), but discussion is controversial for colorectal carcinoma (*33,34*) and breast carcinoma (*35,36*).

CONCLUSION

Data obtained with the multistep targeting technique and PET demonstrated that tumor uptake and tumor to tissue ratios obtained with the enantiomeric Ga chelate are superior to those obtained with the racemic Ga chelate. Thus, with regard to sensitivity of tumor detection, the enantiomeric Ga chelate appears to be more suitable for clinical use despite necessary optical resolution of the naturally racemic Ga chelate preparation. The different in vivo half-lives of the two enantiomeric Ga chelate/BS-MAb immune complexes would offer a choice depending on the renal clearance of the Ga chelate in humans, which, however, is not known at the present. Assuming a slower clearance in humans, the 3A10 containing BS-MAb should be preferred.

Independent of its prognostic value, the VFF18 MAb directed against the human $CD44_{V6}$ already offer a new access for diagnostic or therapeutic targeting of colon, squamous cell and pancreas carcinoma. In combination with the multistep targeting technique and PET, VFF18 containing BS-MAbs should also improve the diagnostic sensitivity for localization of these tumors in patients.

ACKNOWLEDGMENTS

This study was supported by grants from the Tumorzentrum Heidelberg/Mannheim and the Dr. Mildred Scheel Stiftung für Krebsforschung.

REFERENCES

1. Chatal JF, Peltier P, Bardies M et al. Does immunoscintigraphy serve clinical needs effectively? Is there a future for radioimmunotherapy? *Eur J Nucl Med* 1992;19:205–213.
2. Larson SM, Divgi C, Scott A, Daghighian F, Macapinlac H, Welt S. Current status of radioimmunodetection. *Nucl Med Biol* 1994;21:721–729.
3. Bischof-Delaloye A, Delaloye B. Radiolabeled monoclonal antibodies in tumor imaging and therapy: out of fashion? *Eur J Nucl Med* 1995;22:571–580.
4. Larson SM. Improving the balance between treatment and diagnosis: a role for radioimmunodetection. *Cancer Res* 1995;55(suppl):5756s–5758s.
5. Goodwin DA. Tumor pretargeting: almost the bottom line. *J Nucl Med* 1995;36:876–879.
6. Saleh MN, Khazaeli MB, Wheeler RH, et al. Phase I trial of the murine monoclonal anti-GD2 antibody 14G2a in metastatic melanoma. *Cancer Res* 1992;52:4342–4347.
7. Jones PL, Brown BA, Sands H. Uptake and metabolism of ^{111}In labeled monoclonal antibody B6.2 by the rat liver. *Cancer Res* 1990;50(suppl):852s–856s.
8. Jain RK. Physiological barriers to delivery of monoclonal antibodies and other macromolecules in tumors. *Cancer Res* 1990;50(suppl):814s–819s.
9. Juweid M, Neuman R, Paik C, et al. Micropharmacology of monoclonal antibodies in solid tumors: direct experimental evidence for a binding site barrier. *Cancer Res* 1992;52:5144–5153.
10. Goodwin DA, Meares CF, McCall MJ, McTigue M, Chavapong W. Pretargeted immunoscintigraphy of murine tumors with ^{111}In labeled bifunctional haptens. *J Nucl Med* 1988;29:226–234.
11. Le Doussal JM, Gruaz-Guyon A, Martin M, Gautherot E, Delaage M, Barbet J. Targeting of ^{111}In labeled bivalent haptens to human melanoma mediated by bispecific monoclonal antibody conjugates: imaging of tumors hosted in nude mice. *Cancer Res* 1990;50:3445–3452.
12. Paganelli G, Magnani F, Zito E, et al. Three-step monoclonal antibody tumor targeting in carcinoembryonic antigen-positive patients. *Cancer Res* 1991;51:5960–5966.
13. Le Doussal JM, Chetanneau A, Gruaz-Guyon A, et al. Bispecific monoclonal antibody-mediated targeting of an indium-111-labeled DTPA dimer to primary colorectal tumors: pharmacokinetics, biodistribution, scintigraphy and immune response. *J Nucl Med* 1993;34:1662–1671.
14. Philpott GW, Schwarz SW, Anderson CJ, et al. Radioimmuno PET. Detection of colorectal carcinoma with positron-emitting ^{64}Cu-labeled monoclonal antibodies. *J Nucl Med* 1995;36:1818–1824.
15. Schuhmacher J, Klivényi G, Matys R, et al. Multistep tumor targeting in nude mice using bispecific antibodies and a gallium chelate suitable for immunoscintigraphy with positron emission tomography. *Cancer Res* 1995;55:115–123.

16. Zöller M, Schuhmacher J, Reed J, Maier-Borst W, Matzku S. Establishment and characterization of monoclonal antibodies against an octahedral galliumchelate suitable for immunoscintigraphy with PET. *J Nucl Med* 1992;33:1366–1372.
17. Heider KH, Sproll M, Susanis S, et al. Characterization of a high-affinity monoclonal antibody specific for $CD44_{v6}$ as candidate for immunotherapy of squamous cell carcinomas. *Cancer Immunol Immunother* 1996;43:245–253.
18. Günthert U. CD44 in malignant disorders. *Curr Top Microbiol Immunol* 1996;213: 271–285.
19. Rall CJN, Rustgi AK. CD44 isoform expression in primary and metastatic pancreatic adenocarcinomas. *Cancer Res* 1995;55:1831–1835.
20. Günthert U. CD44: a multitude of isoforms with diverse functions. *Curr Top Microbiol Immunol* 1993;184:47–63.
21. Parham P, Androlewicz MJ, Brodsky FM, Holnus NJ, Ways JP. Monoclonal antibodies: purification, fragmentation and application to structural and functional studies of class I MHC antigens. *J Immunol Methods* 1982;53:133–173.
22. Lamoyi E, Nisonoff A. Preparation of $F(ab)_2$ fragments from mouse IgG of various subclasses. *J Immunol Methods* 1983;56:235–243.
23. Fogh J, Trempe G. New human tumor cell lines. In: Fogh J, ed. *Human tumor cells in vitro.* New York: Plenum Press; 1975:115–159.
24. Hofmann M, Rudy W, Zöller M et al. CD44 splice variants confer metastatic behaviour in rats: homologous sequences are expressed in human tumor cell lines. *Cancer Res* 1991;51:5292–5297.
25. Schuhmacher J, Maier-Borst W. A new $^{68}Ge/^{68}Ga$ radioisotope generator system for production of ^{68}Ga in dilute HCl. *Int J Appl Radiat Isot* 1981;32:31–36.
26. Lindmo T, Boven E, Cuttita F, Fedorko J, Bunn PA. Determination of the immunoreactive fraction of radiolabeled monoclonal antibodies by linear extrapolation to binding at infinite antigen excess. *J Immunol Methods* 1984;72:77–89.
27. Badger CC, Krohn KA, Bernstein ID. *In vitro* measurement of avidity of radioiodonated antibodies. *Nucl Med Biol* 1987;14:605–610.
28. Doll J, Brix G, Bellemann ME, et al. Improvement of spatial resolution in PET by implementing scanner characteristics in iterative image reconstruction algorithms. In: Richter J, ed. *Medizinische physik 1995. Jahrestagung der deutschen gesellschaft für medizinische physik.* Frankfurt: Linea Plus Druck; 1995:322–323.
29. Stewart M. Antigenerkennung. In: Roitt IM, Brostoff J, Male DK, eds. *Immunologie,* 2nd ed. Stuttgart: Georg Thieme Verlag; 1991:79–89 (German translation, Harabacz I).
30. Goodwin DA, Meares CF, McTigue M, et al. Pretargeted immunoscintigraphy: effect of hapten valency on murine tumor uptake. *J Nucl Med* 1992;33:2006–2013.
31. Günthert U, Hofmann M, Rudy W, et al. A new variant of glycoprotein CD44 confers metastatic potential to rat carcinoma cells. *Cell* 1991;65:13–24.
32. Stauder R, Eisterer W, Thaler J, Günthert U. CD 44 variant isoforms in non-Hodgkin's lymphoma: a new independent prognostic factor. *Blood* 1995;85:2885–2889.
33. Mulder JWR, Kruyt PM, Sewnath M, et al. Colorectal cancer prognosis and expression of exon-v_6-containing CD44 proteins. *Lancet* 1994;344:1470–1472.
34. Koretz K, Möller P, Lehnert T, Hinz H, Otto HF, Herfahrt C. Effect of $CD44_{v6}$ on survival in colorectal carcinoma. *Lancet* 1995;345:327–328.
35. Kaufmann M, Heider KH, Sinn HP, Minckwitz G, Ponta H, Herrlich P. CD44 variant exon epitopes in primary breast cancer and length of survival. *Lancet* 1995;345:615–619.
36. Friedrichs K, Franke F, Lisboa BW, et al. CD44 isoforms correlate with cellular differentiation but not with prognosis in human breast cancer. *Cancer Res* 1995;55: 5424–5433.

EDITORIAL

Bullets to Magic Bullets—and Miles to Go Before We Sleep

In this issue of the *Journal of Nuclear Medicine*, Klivényi et al. (*1*) highlight the advantages and limitations in their studies of pretargeting xenografted tumor using a bispecific antitumor/antihapten antibody followed by ^{68}Ga chelate. They report that the system permits excellent PET imaging; importantly, they delineate the effect of enantiomer selection on tumor uptake and tumor-to-nontumor ratios.

The need to improve relative uptake of radionuclide in tumor using an antibody-based targeting system is urgent. The clearance of intact immunoglobulins is slow, resulting in low target-to-background ratios, especially early after administration, thereby limiting the use of nuclide-based detection and therapy. The considerable advantages of PET have intensified efforts to develop antibody-mediated tumor imaging methods appropriate for use with short-lived positron emitters. Rapid tumor localization is also essential in targeted therapy using short-lived alpha-emitting isotopes.

Seminal studies, using antichelate antibodies followed by a radiolabeled chelate (*2*) and various avidin–biotin approaches (*3*), showed the potential of pretargeting a decade ago. Since then, the technique has been refined in many aspects, several of which were used in the present study. Examples include the evaluation of various bifunctional antibody constructs with mono- or bivalent binding to tumor antigen (*4–6*), the application of blood-clearing agents to remove circulating antibodies before injection of effector molecule; and the use of bivalent hapten molecules, which apparently enhance tumor uptake (*4,7*). A clinical study in colorectal cancer patients demonstrated significantly improved tumor-to-nontumor ratios when comparing bifunctional antibody/^{111}In-diethylenetriamine pentaacetic acid (DTPA) with its bivalent ^{111}In-labeled counterpart (*8*), underscoring the potential of the method.

The avidin–biotin system has the advantage of the extremely high affinity (10^{-15} M) between biotin and the proteins avidin and streptavidin and the possibility of enhancing tumor signal, because both avidin and streptavidin have four binding sites for biotin, the preferred effector molecule. Grana et al. (*9*) successfully showed the use of their three-step targeting approach; biotinylated antibody followed by avidin/streptavidin and finally radiolabeled biotin, in a variety of solid tumors. The most extensive clinical trial evaluating pretargeting for therapy has been initiated by NeoRx (Seattle, WA). A pretargeted streptavidinylated antibody is followed by a clearing agent, after which biotin, labeled with ^{90}Y by the metal chelator 1,4,7,10-tetrazacyclododecane-1,4,7,10-tetraacetic acid (DOTA), is administered. Initial clinical trials from both groups have shown that the amount of radioactivity that can be safely administered is significantly greater with this methodology than with radiolabeled antibody alone (*10,11*).

An interesting alternative to the antibody/hapten and avidin–biotin systems, presented by Hnatowich et al. (*12*), is the use of peptide nucleic acid (PNA). The interaction between complementary PNA strands is essentially similar to that of deoxyribonucleic acid, but the peptide backbone of PNA results in greater serum stability, increasing the applicability of single-strand radiolabeled PNA to localize tumor that is pretargeted with an antibody conjugated with the complementary PNA strand. Regardless of the choice of "receptor-ligand" pair, the selection of an appropriate antibody–antigen system is imperative, perhaps more so in pretargeting techniques than in conventional radioimmunotargeting. The complexity of the system necessitates careful optimization.

Pretargeting has also found applications outside the realm of nuclear medicine. Antibody-directed prodrug therapy, in which an antibody is used to direct an enzyme to the tumor site where it can subsequently convert a prodrug to a cytotoxic agent, is in clinical trials (*13*). In addition, bispecific antibodies that recognize tumor-associated antigens and immune effector antigens have been studied as immunotherapeutic agents. Initial studies used anti-CD3 antibodies (*14*); later studies have targeted the constant fragment gamma receptor family (*15*),

Received Jul. 17, 1998; revision accepted Aug. 4, 1998.
For correspondence or reprints contact: Chaitanya Divgi, MD, Memorial Sloan-Kettering Cancer Center, 1275 York Ave., New York, NY 10021.